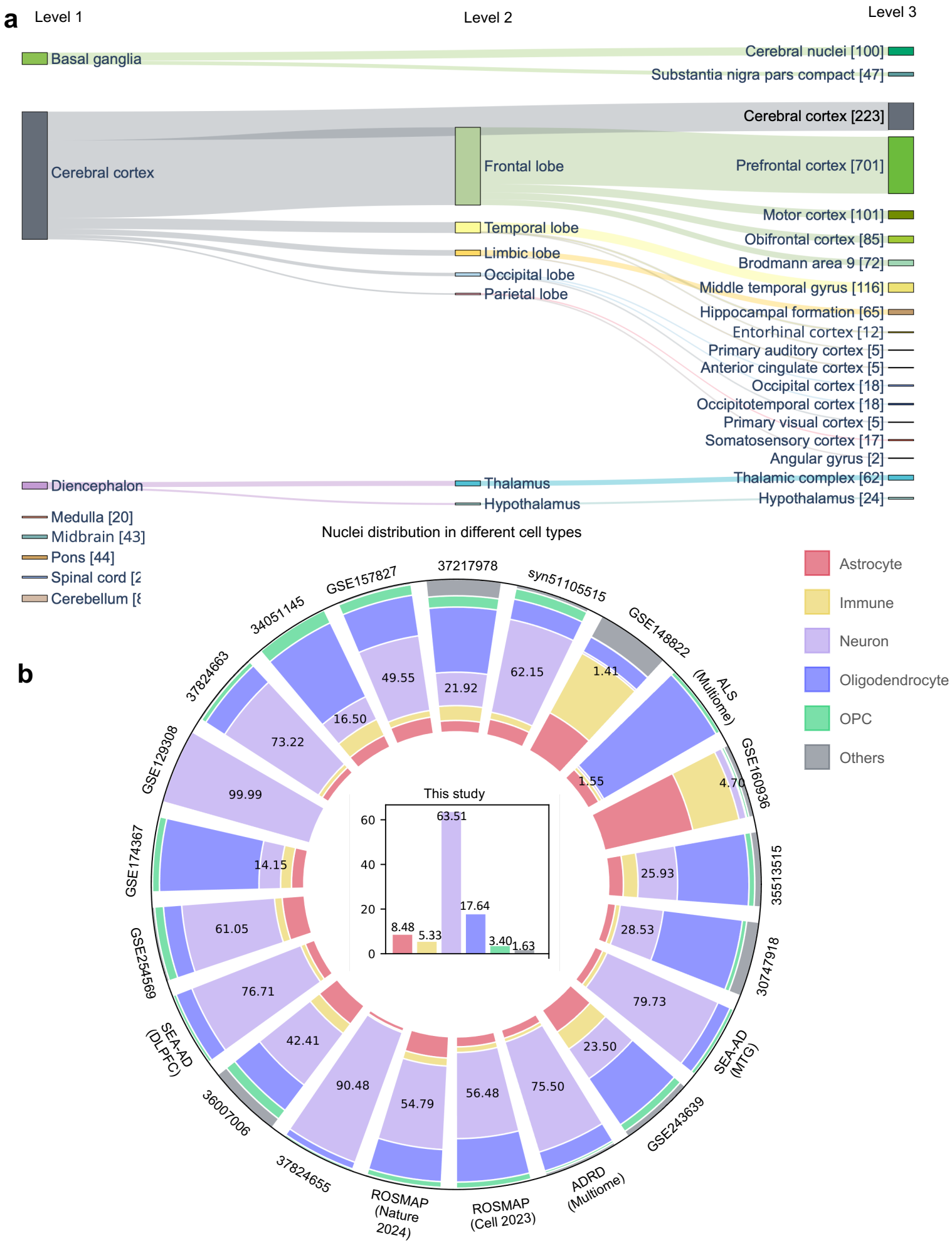

Supplemental Figure S1. Additional meta information for the atlas (a). Hierarchical structures for all brain regions considered in this atlas **(b).** Cell type distributions across all datasets in the atlas.

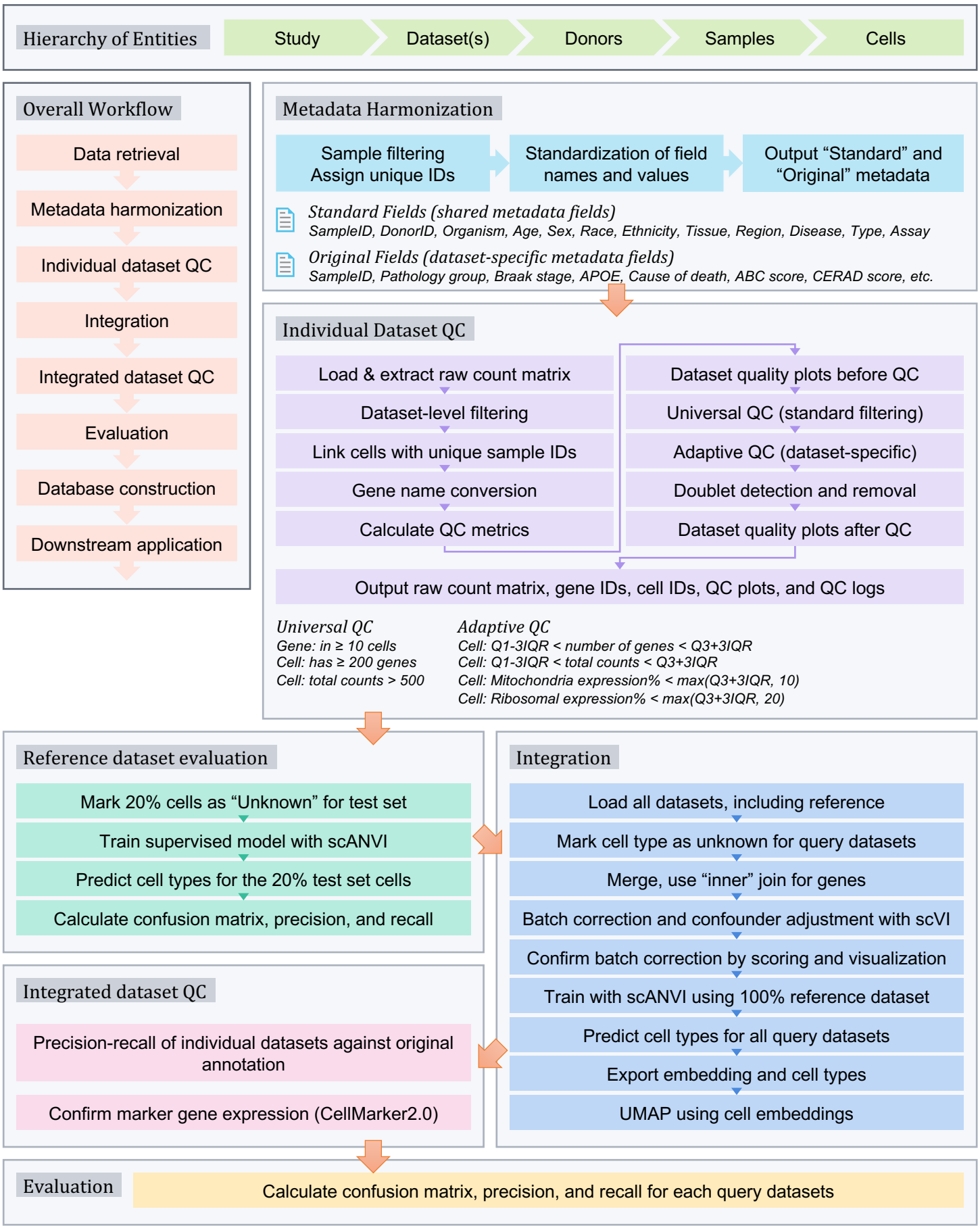

Supplemental Figure S2. Detailed workflow for building the atlas (including data collection, data quality control, metadata and RNA-seq data harmonization).

Supplemental Figure S3: Dot plots of marker genes for (a). all Level 1 cell types and (b). all Level 2 neuron subtypes.

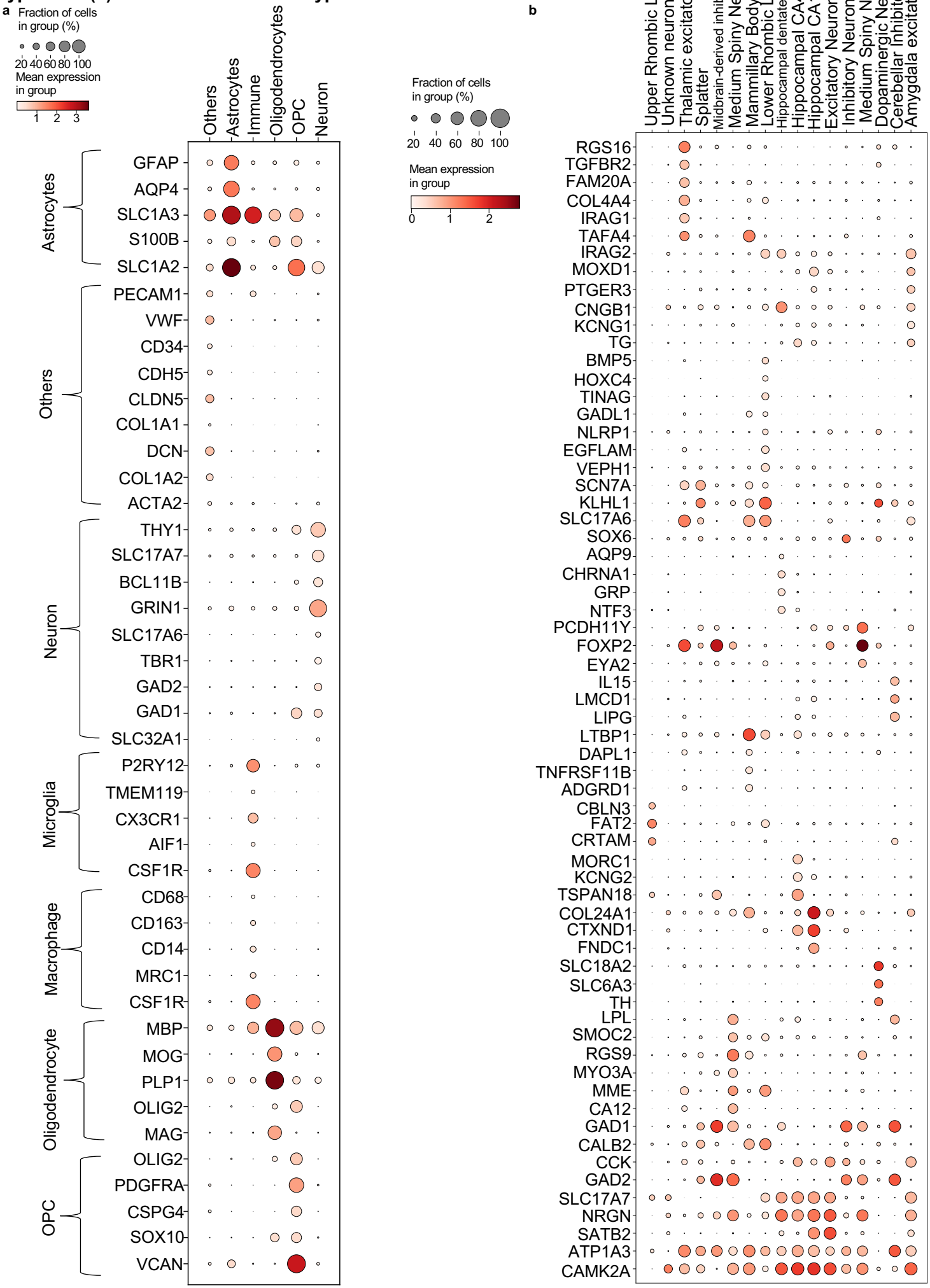

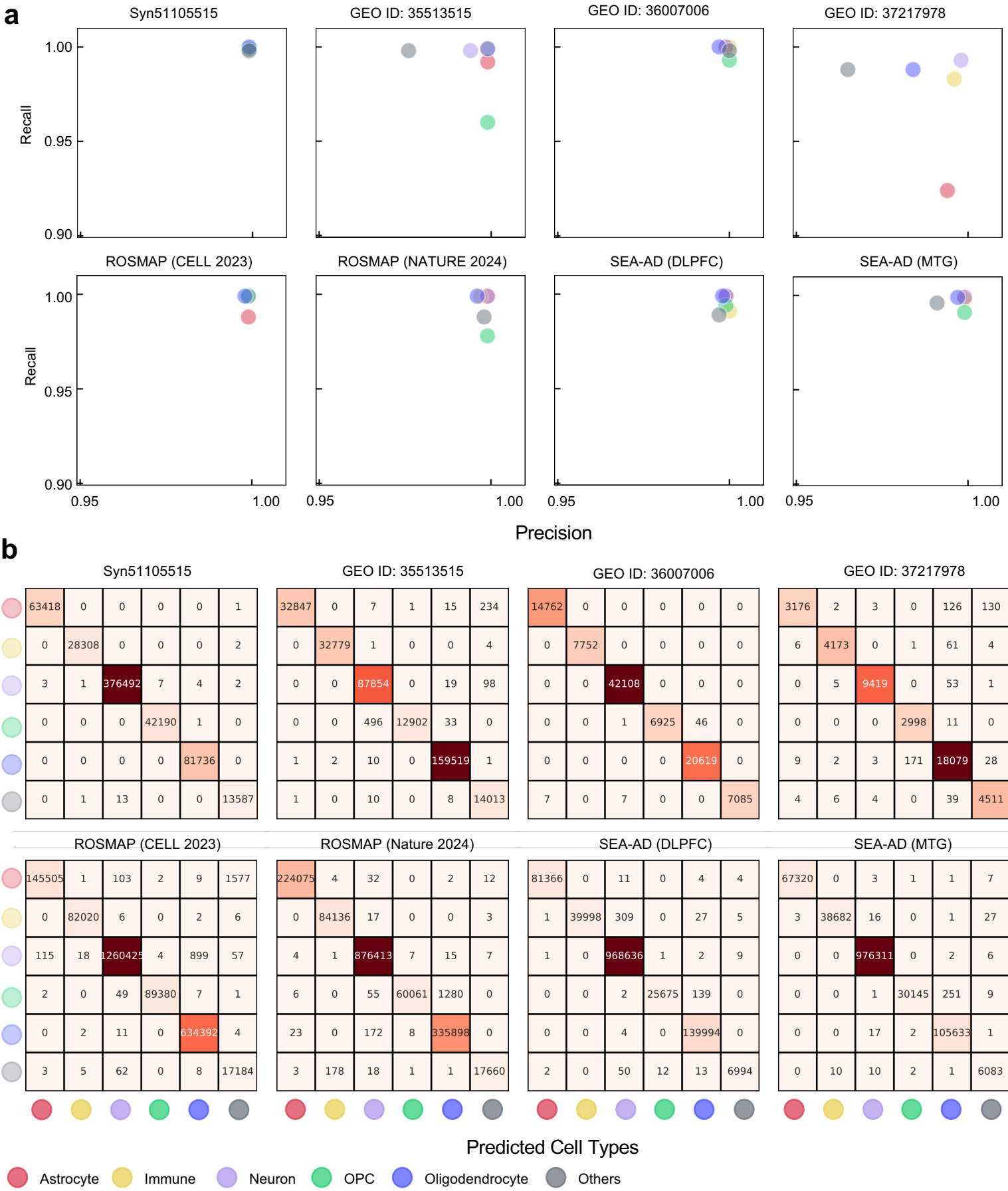

Supplemental Figure S4. Consistency evaluation for harmonized and original Level 1 cell type annotations for multiple datasets considering (a). precision and recall values and **(b).** confusion matrices.

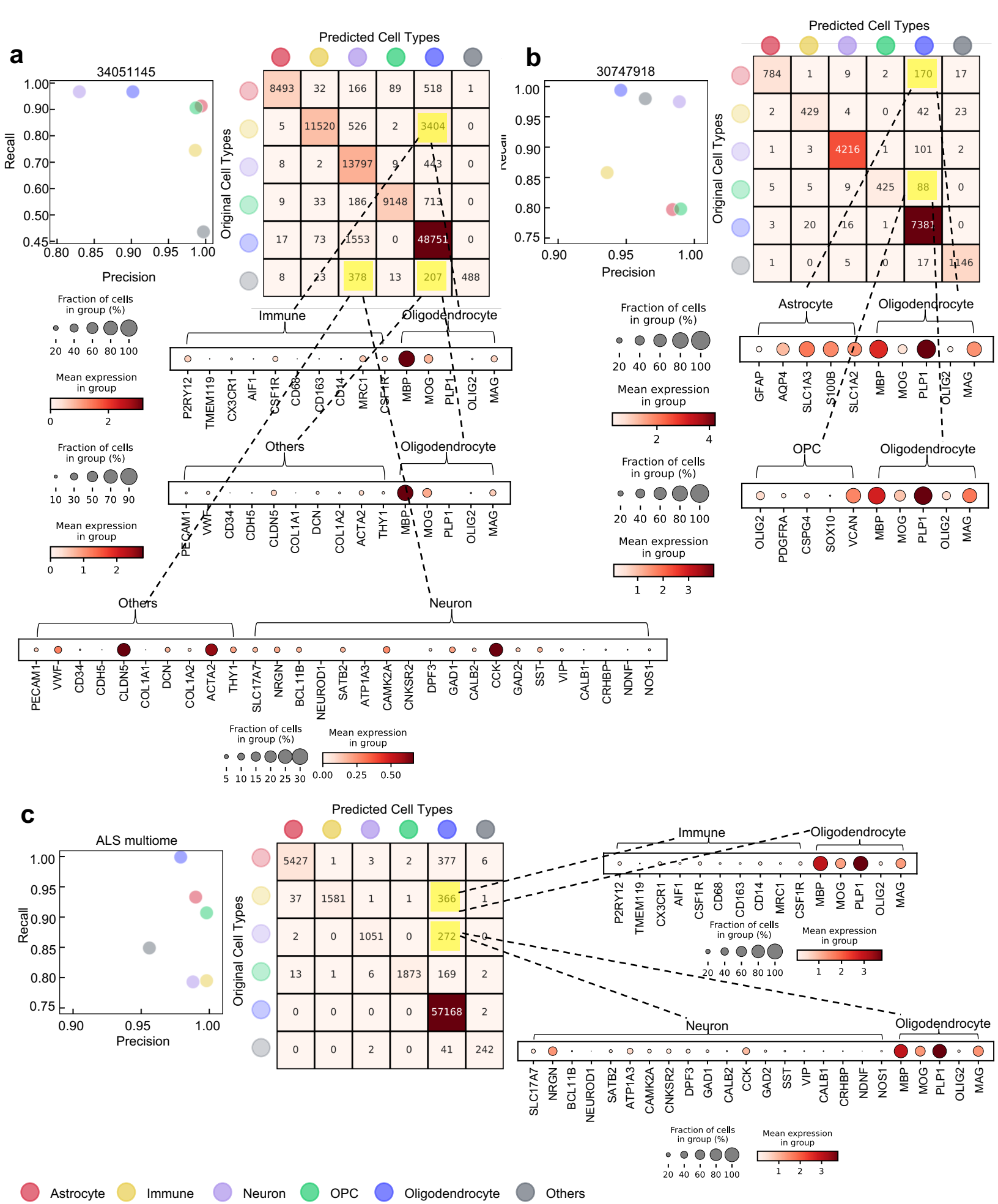

Supplemental Figure S5. Additional analyses for unmatched Level 1 cell type annotations between harmonized atlas and original studies via independent cell type marker database CellMarker2.0 for datasets (a). GEO ID: 34051145, **(b). GEO ID:** 30747918, and **(c).** ALS_multiome.

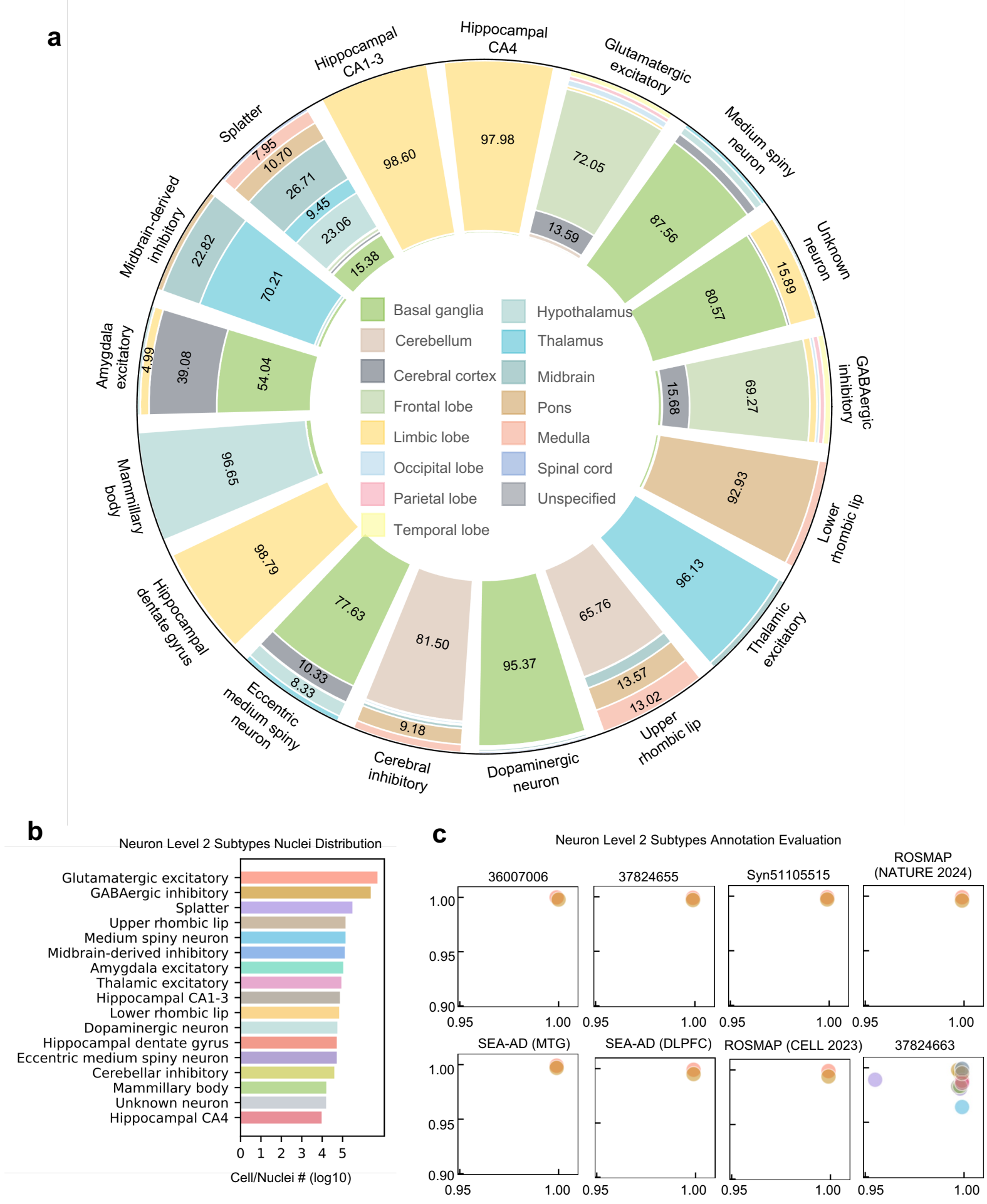

Supplemental Figure S6. Additional information of harmonized neuron Level 2 subtypes (a). Cellular abundance distributions (percentages) across brain regions; **(b).** Nuclei population (log10 scale); **(c).** Consistencies (i.e., precision and recall) between harmonized and original neuronal Level 2 subtype annotations.

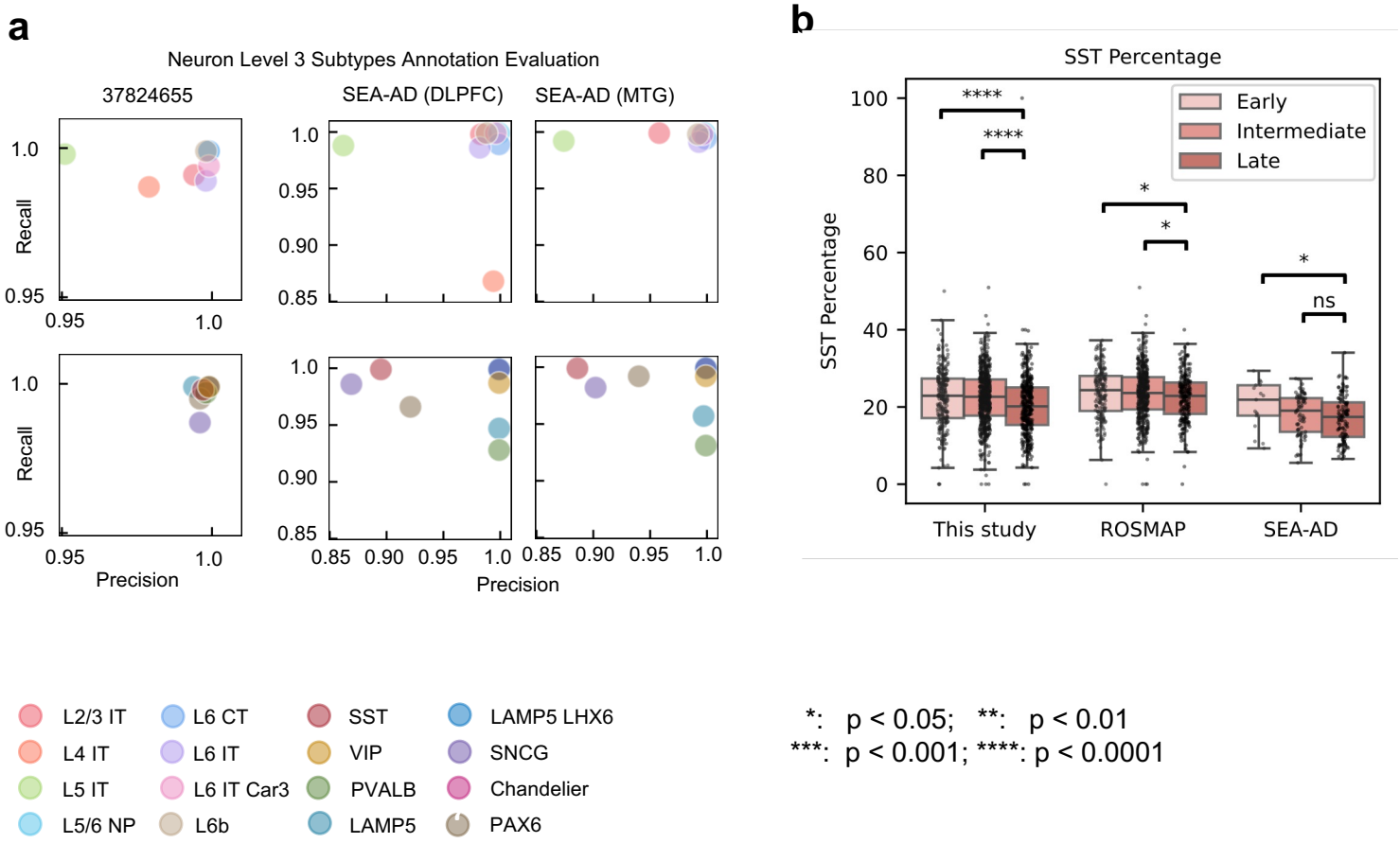

*: $p < 0.05$; **: $p < 0.01$
***: $p < 0.001$; ****: $p < 0.0001$

Supplemental Figure S7. Additional information of harmonized neuron Level 3 subtypes (a). Consistencies (i.e., precision and recall) between harmonized and original neuronal Level 3 subtype (i.e., glutamatergic and GABAergic neurons) annotations. **(b).** The cellular abundance distribution of SST neurons across different disease stages when considering the entire harmonized atlas and two independent cohorts: ROSMAP and SEA-AD.

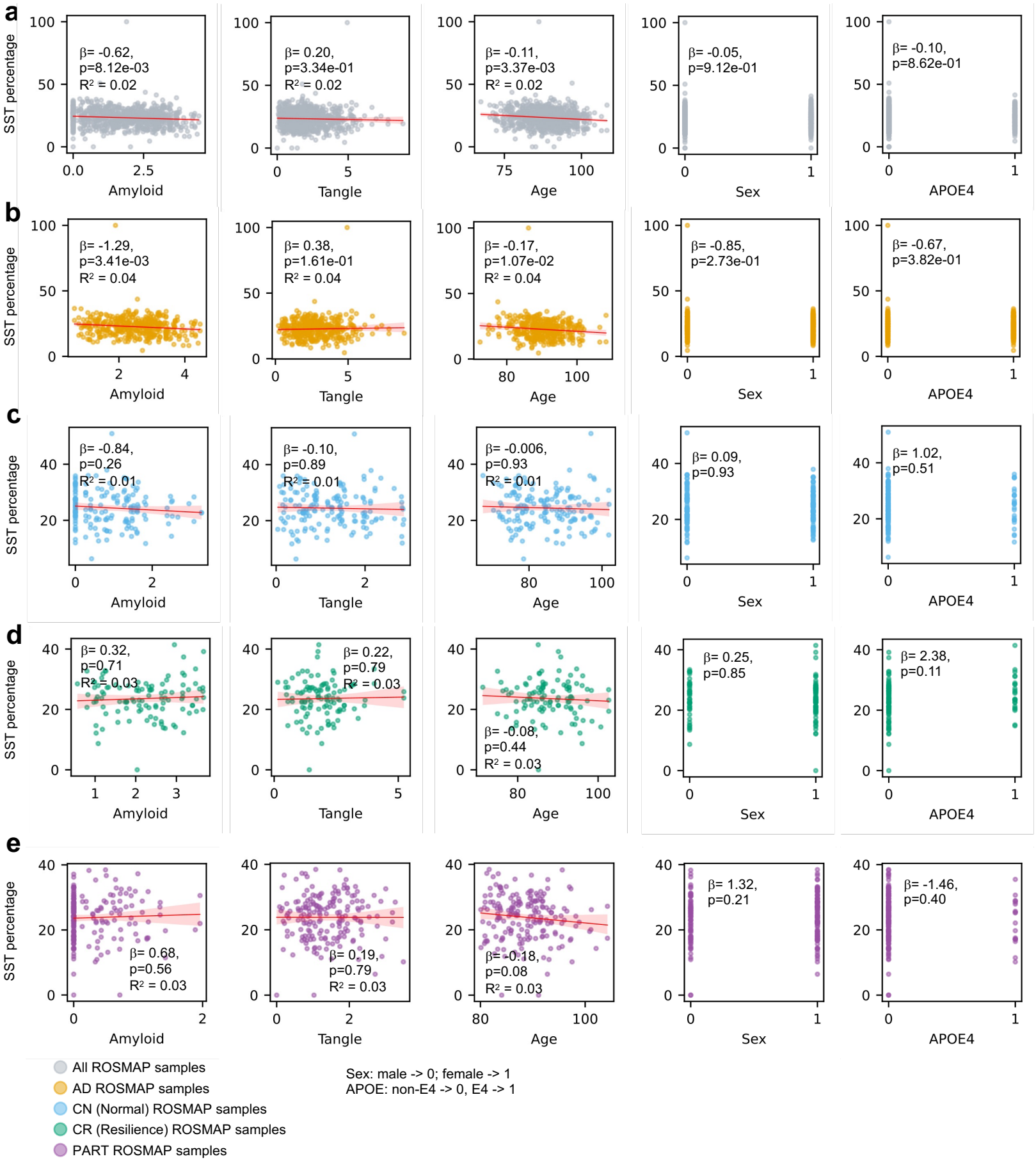

Supplemental Figure 8. Correlations between cellular abundance of SST neuron and five clinical categories (i.e., amyloid plaque and tau tangle densities, age, sex and APOE4 genotype) when considering the entire atlas and its four deeply harmonized subgroups (i.e., AD, CN, CR and PART).

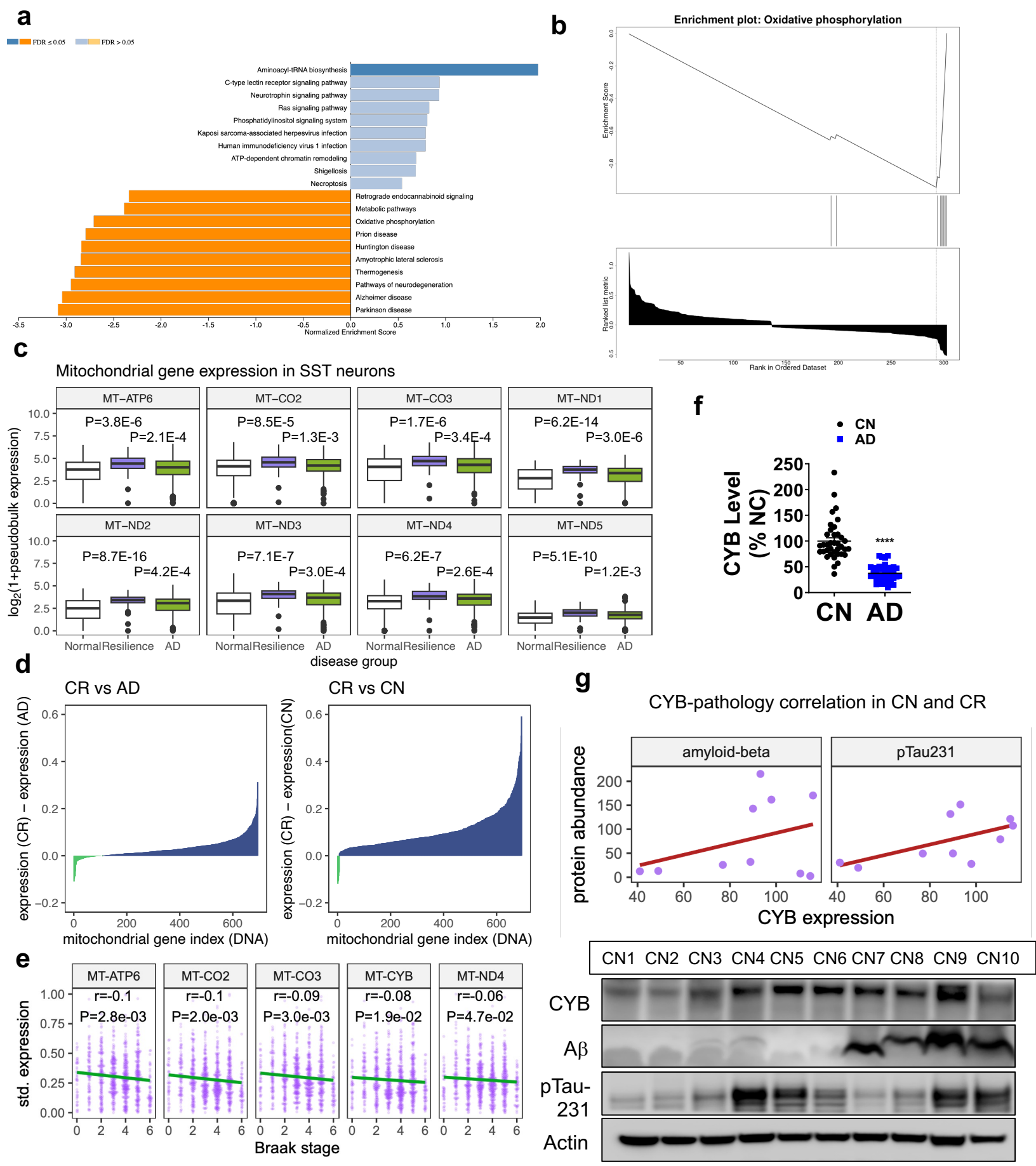

Supplemental Figure S9. Additional information of SST neurons associated with cognitive resilience (a). Pathway enrichment results for SST neuron specific DEGs **(b).** GSEA enrichment results for SST neuron specific DEGs **(c).** Eight mitochondrial gene expressions in SST neuron when compared in CN (normal), CR (resilience) and AD groups. **(d).** Expression differences of nuclear-encoded genes that function in mitochondria when compared between CR (resilience) and AD and between CR (resilience) and CN (normal). **(e).** Correlations between gene expressions and braak stages for five mitochondria genes (i.e., MT-ATP6, MT-CO2, MT-CO3, MT-CYB, and MT-ND4). **(f).** Quantification of MT-CYB in both CN (normal) and AD brain samples (t-test, n = 5 for each group, p = 1.1×10^{-19}). **(g).** Correlation of protein abundances between MT-CYB and amyloid-beta and pTau-231 in CN (normal) brain samples. Western-blot for MT-CYB levels with different Aβ and pTau-231 levels.

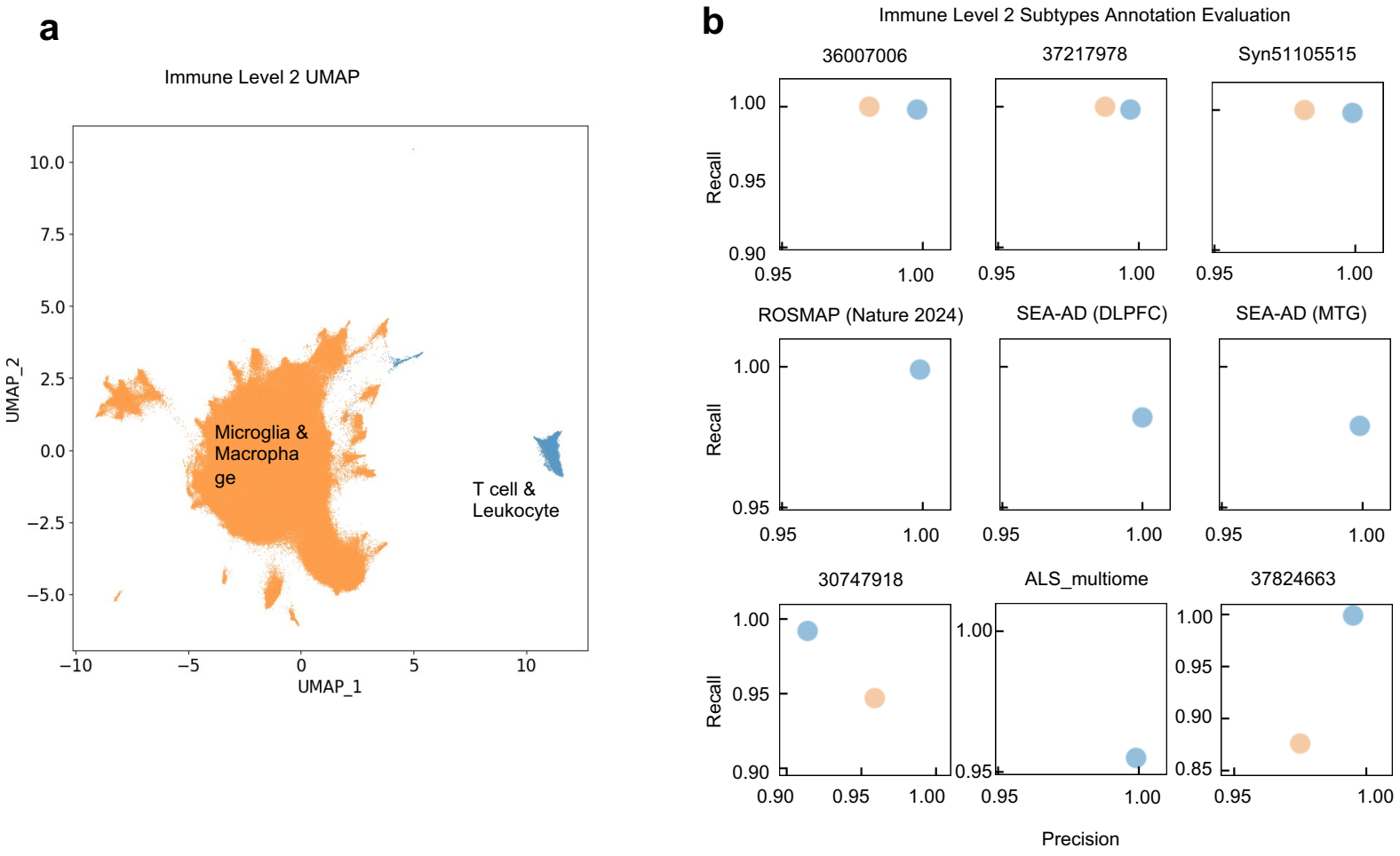

Supplemental Figure S10. Additional information of harmonized immune Level 2 subtypes (a). Uniform Manifold Approximation and Projection (UMAP) of immune Level 2 subtypes 'Microglia & Macrophage' and 'Tcells & Leukocytes' **(b).** Consistencies (i.e., precision and recall) between harmonized and original immune Level 2 subtype annotations.

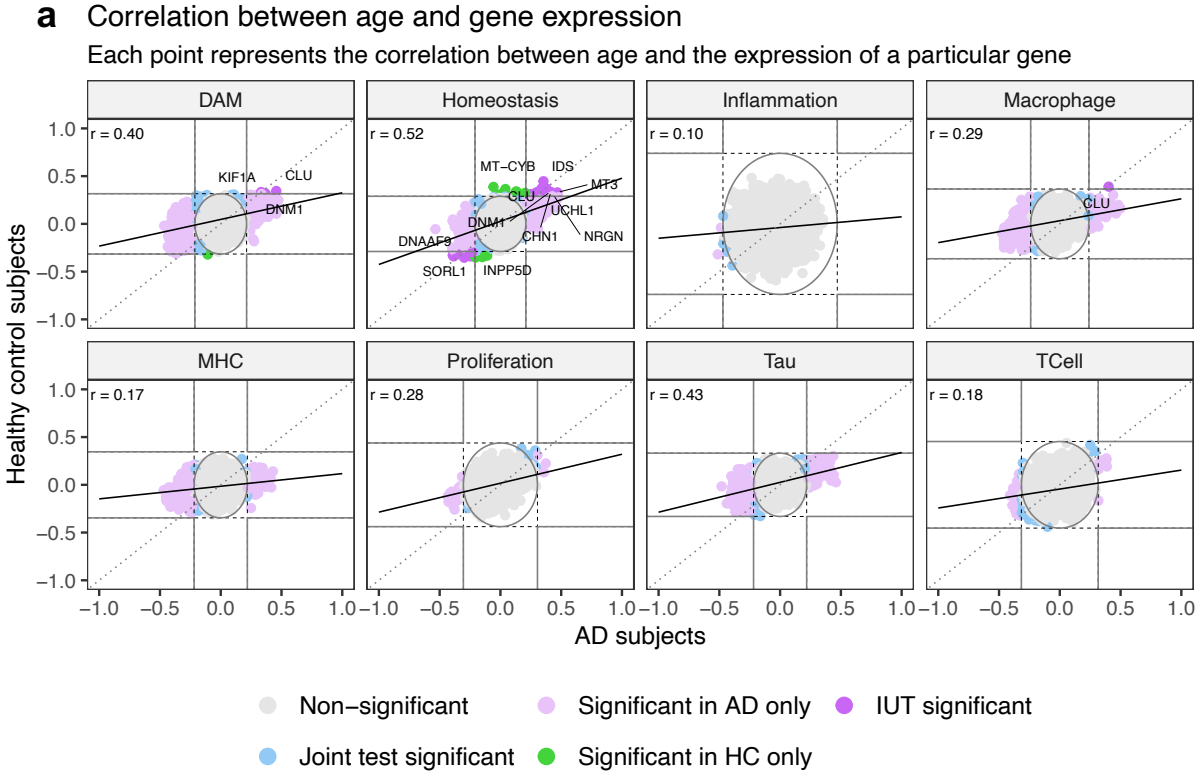

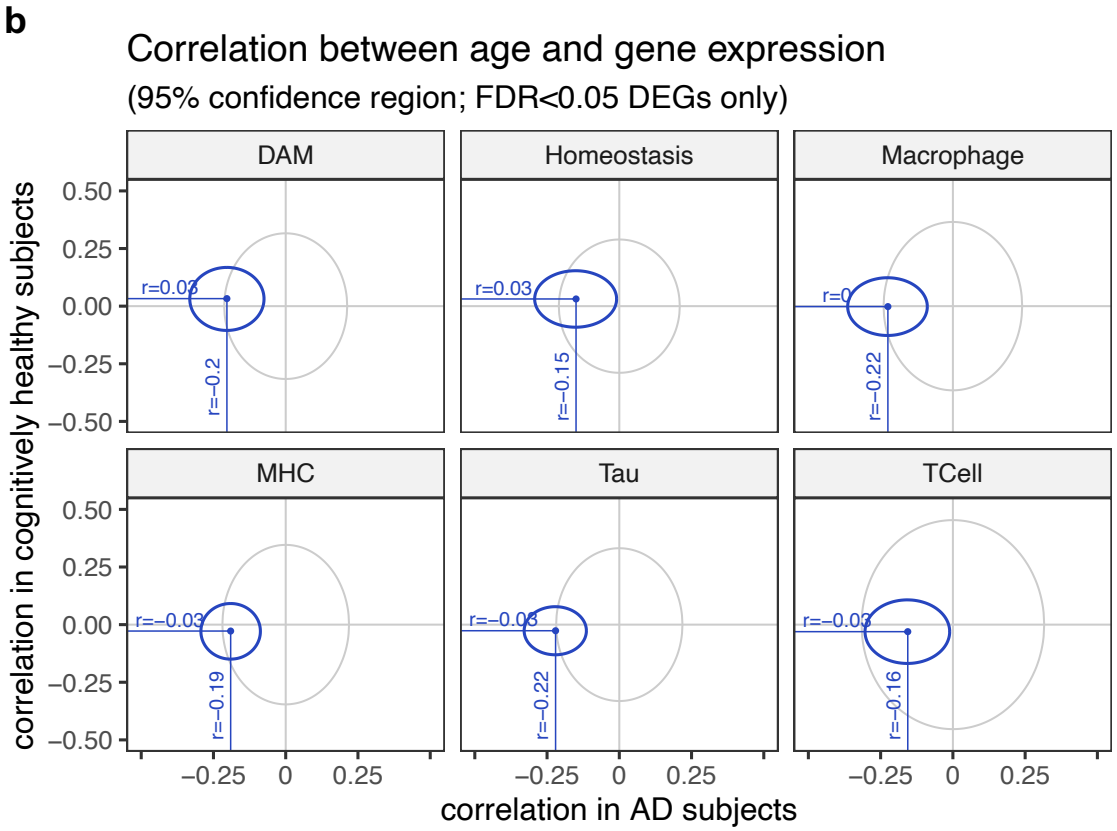

Supplemental Figure S11. Additional information of immune aging clock. (a). Correlations between age and gene expressions for both CN (normal) and AD subjects when considering multiple immune Level 3 subtypes. **(b).** Modal correlations between age and gene expressions for both CN (normal) and AD subjects considering three immune Level 3 subtypes (i.e., disease-associated microglial [DAM], homeostatic microglia and macrophage).

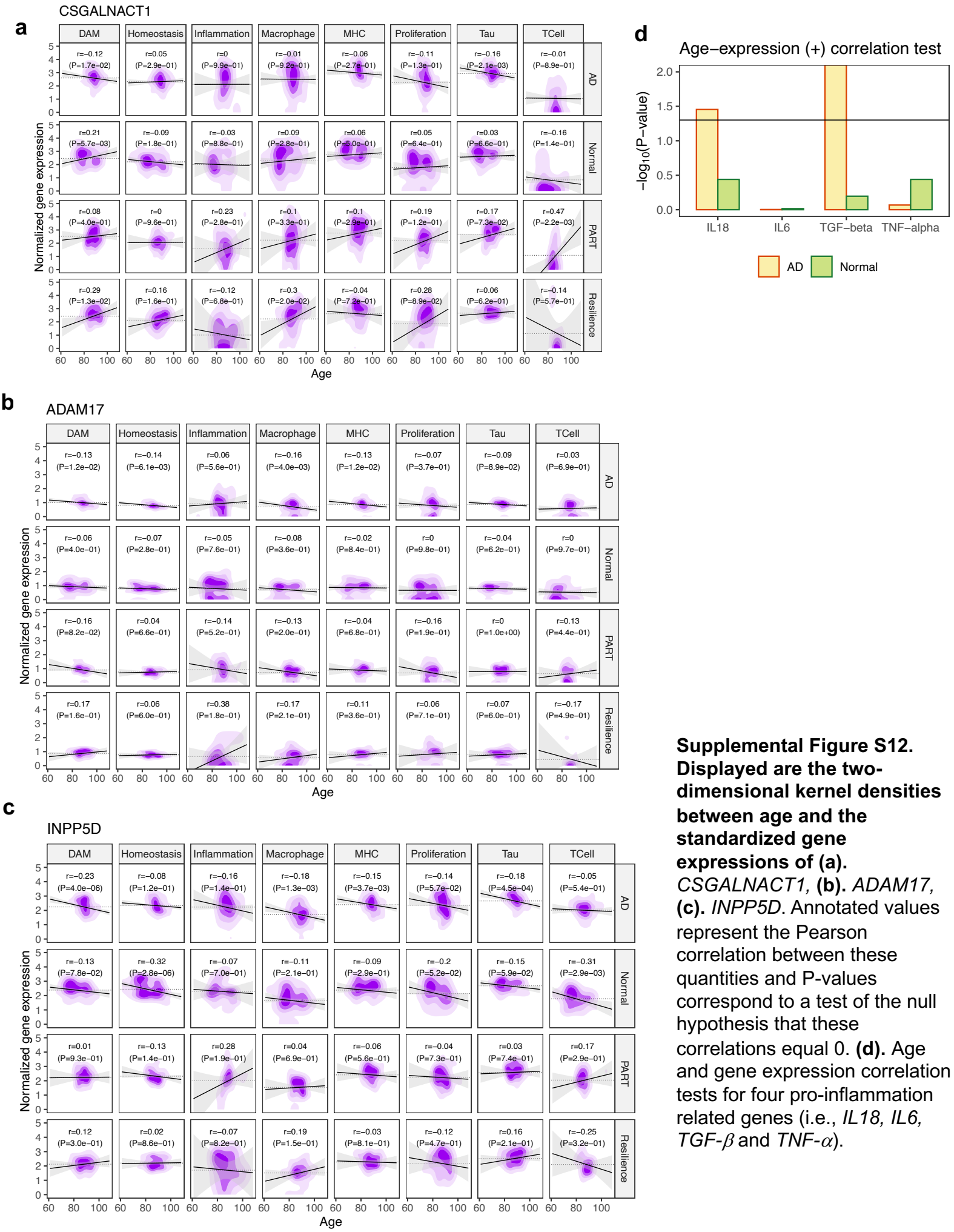

Supplemental Figure S12. Displayed are the two-dimensional kernel densities between age and the standardized gene expressions of (a). *CSGALNACT1,* **(b).** *ADAM17,* **(c).** *INPP5D*. Annotated values represent the Pearson correlation between these quantities and P-values correspond to a test of the null hypothesis that these correlations equal 0. **(d).** Age and gene expression correlation tests for four pro-inflammation related genes (i.e., *IL18, IL6, TGF-β* and *TNF-α*).

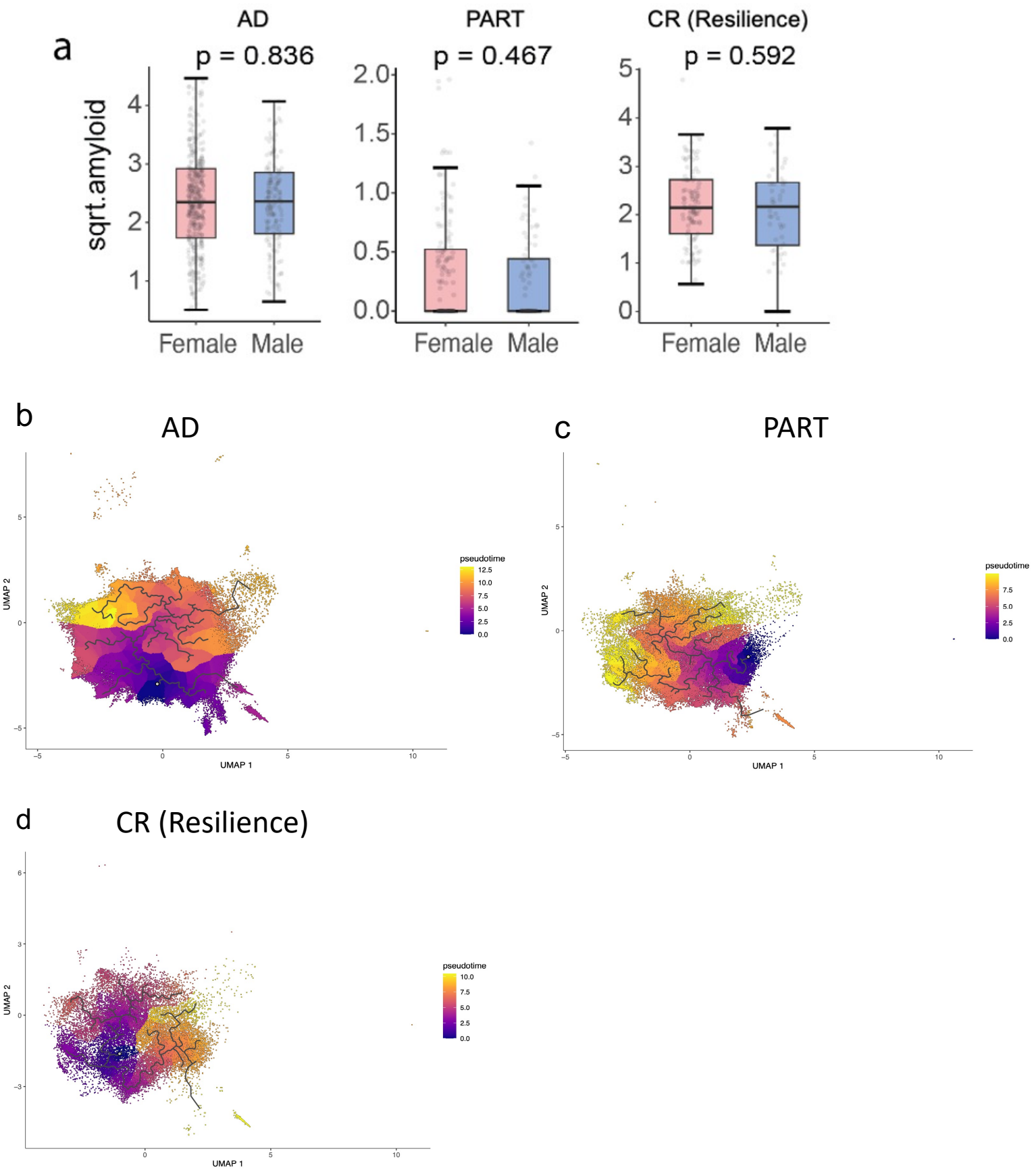

Supplemental Figure S13. Additional information of sex differences in neuropathological changes in AD, PART, and CR. (a). Density of amyloid comparison between male and female individuals across AD, PART and CR (Resilience) groups. Trajectories generated with monocle3 for **(b)** AD, **(c)** PART and **(d)** CR (Resilience) groups.

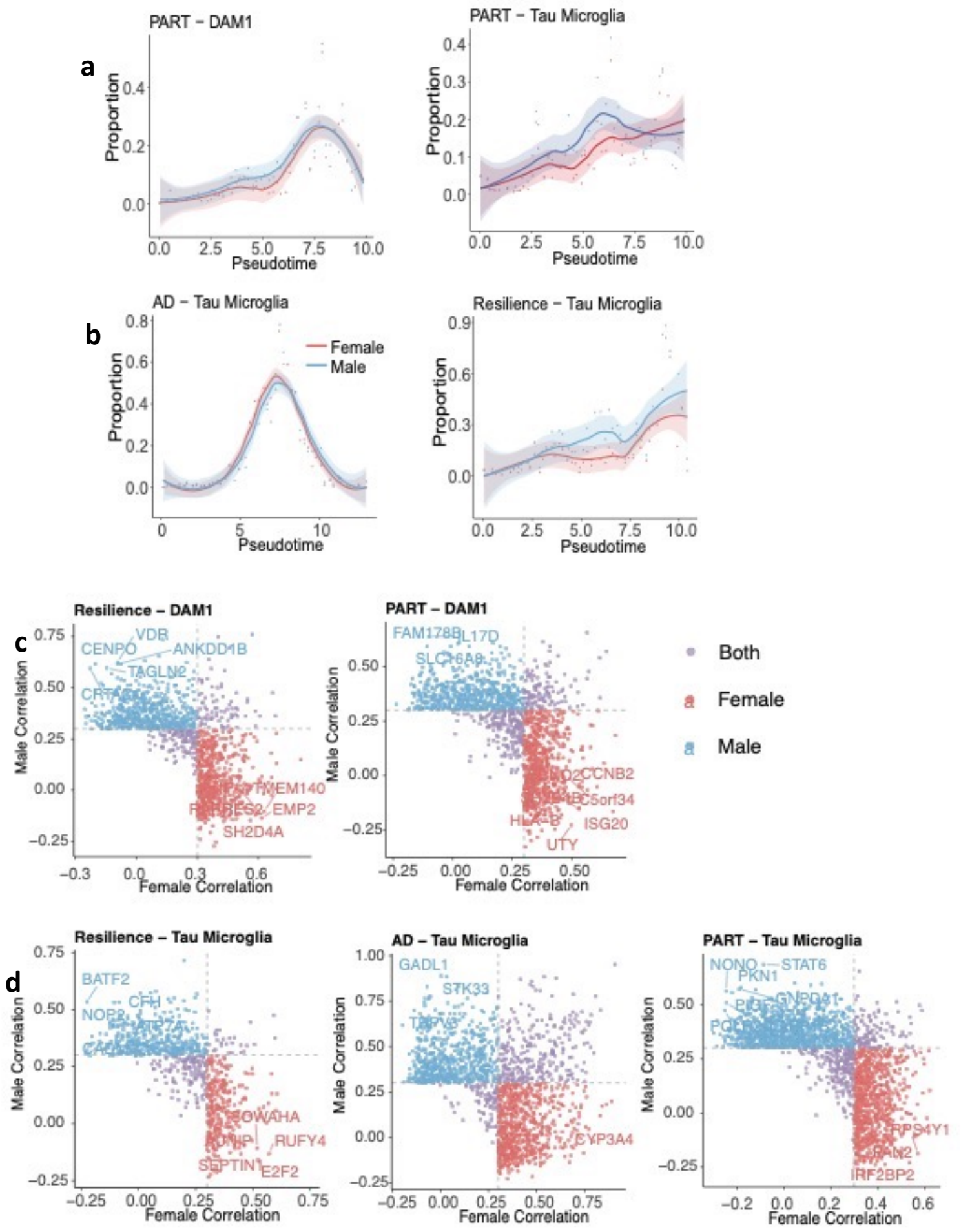

Supplemental Figure S14. Additional information of sex differences in neuropathological changes in AD, PART, and CR. (a). Cell type (i.e., DAM1 and tau microglia) proportions along microglia trajectory in PART group considering both male and female subjects. **(b).** Cell type (i.e., tau microglia) proportions along microglia trajectory in both AD and CR (Resilience) groups considering both male and female subjects. Heatmap of sex-specific driver genes across microglial trajectory for **(c)** DAM1 in PART and CR (Resilience) groups and **(d)**. tau microglia in CR (Resilience), AD and PART groups.

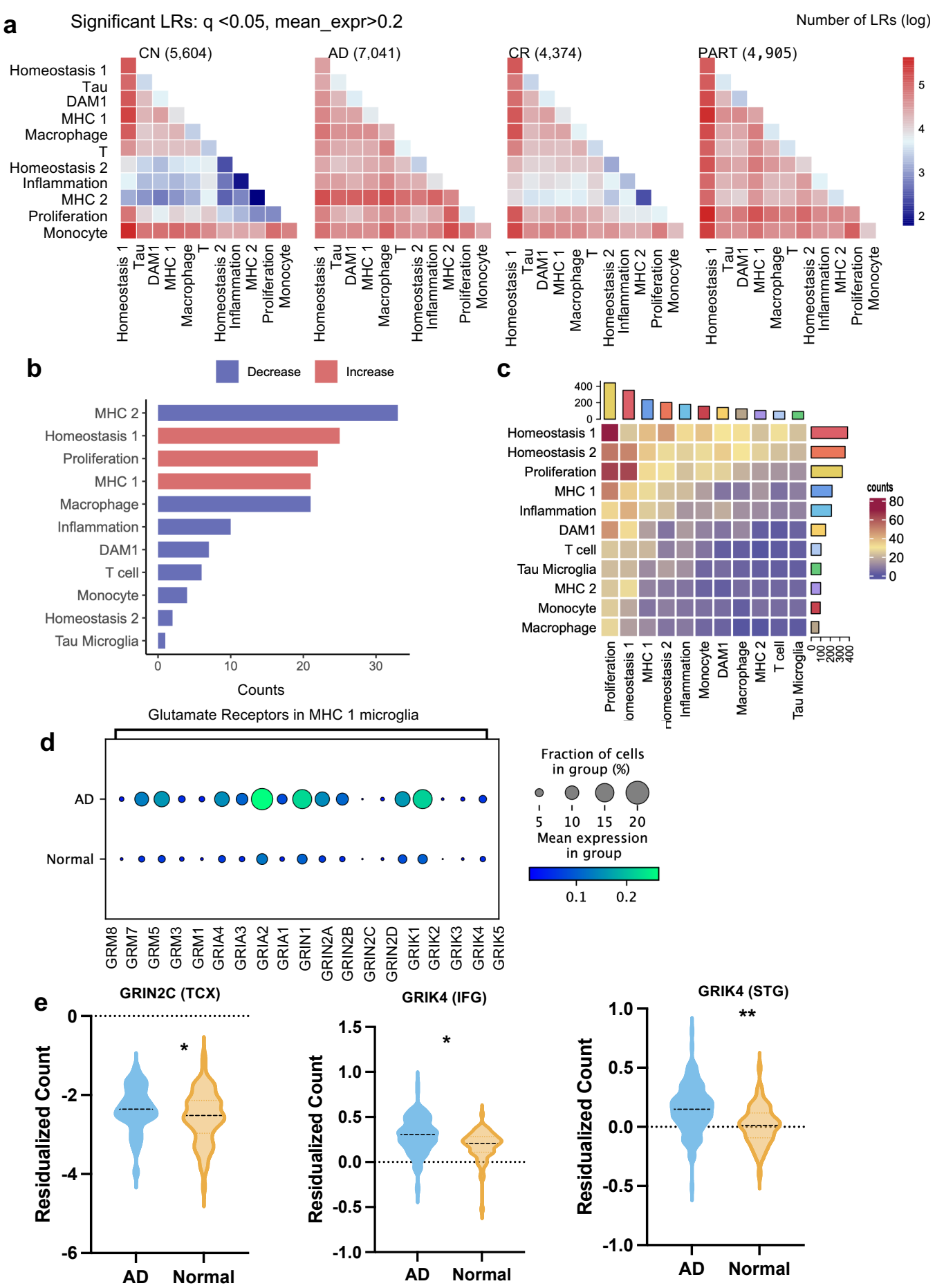

Supplemental Figure S15. Cellular community within immune subpopulations across different groups (a). The number of inferred interactions (LRs) among immune subpopulations. From left to right: CN, AD, CR, and PART groups (q < 0.05, mean_expr > 0.2). **(b).** Bar plots showing differential interactions from T cell to microglial subpopulations (AD vs. CN). **(c).** Heatmap showing AD specific LRs (AD vs. CN/CR). **(d).** Dot plots showing the gene expression of glutamate receptors in MHC 1 microglia. **(e).** Violin plots showing the differential expression of selected glutamate receptors in bulkRNA-seq data (AD vs. CN, * q <0.05; ** q<0.01; *** q < 0.0001). TCX: temporal cortex; IFG: inferior frontal gyrus; STG: superior temporal gyrus.

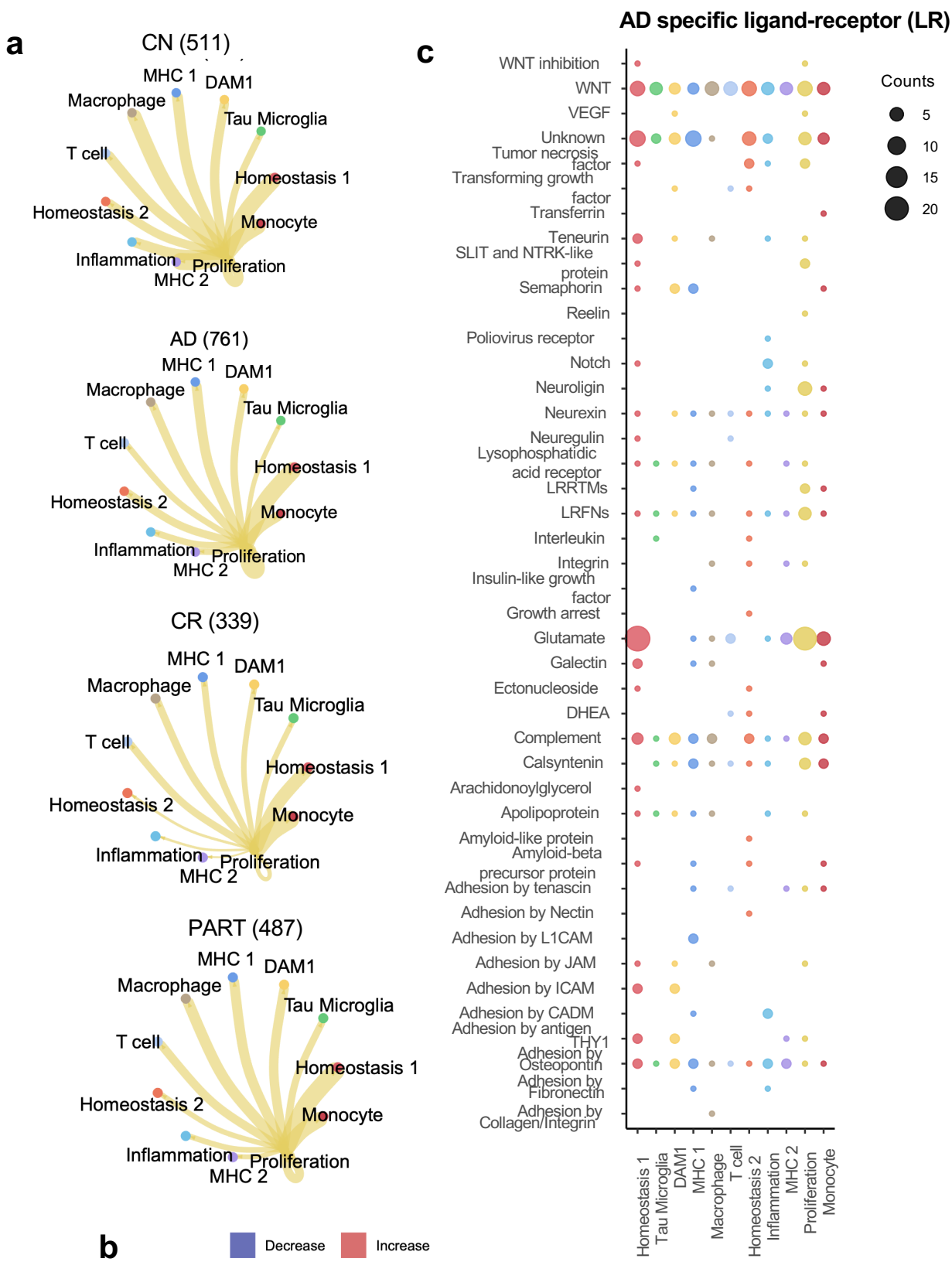

Supplemental Figure S16. Cellular community in proliferation microglia across different groups (a). Circle plots showing interactions (LRs) in proliferation microglia across different groups. Up to down: CN, AD, CR and PART. **(b).** Bar plots showing differential interactions from proliferation cell to immune subpopulations (AD vs. CR). **(c).** Dot plots showing AD-specific LRs from proliferation microglia to different immune subpopulations (AD vs. CN/CR).

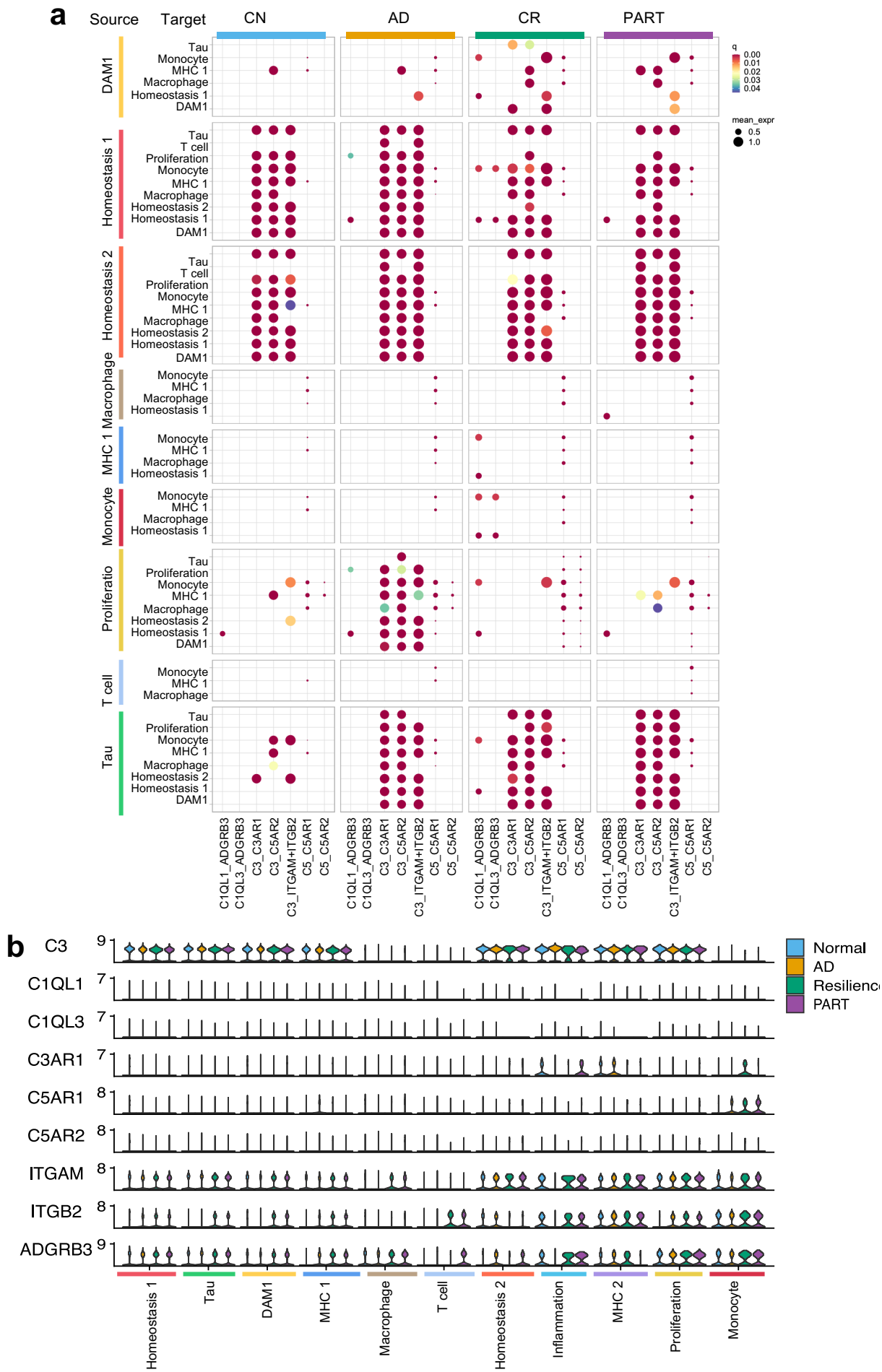

Supplemental Figure S17. Signal of complement across different groups (a). Dot plots showing signal of complement within different immune subpopulations across different immune subpopulations. **(b).** Violin plots showing expression of LRs within complement signal across different immune subpopulations. Ligands: C3, C1QL1, C1QL3; Receptors: C3AR1, C5AR1, C5AR2, ITGAM. ITGB2, ADGRB3.

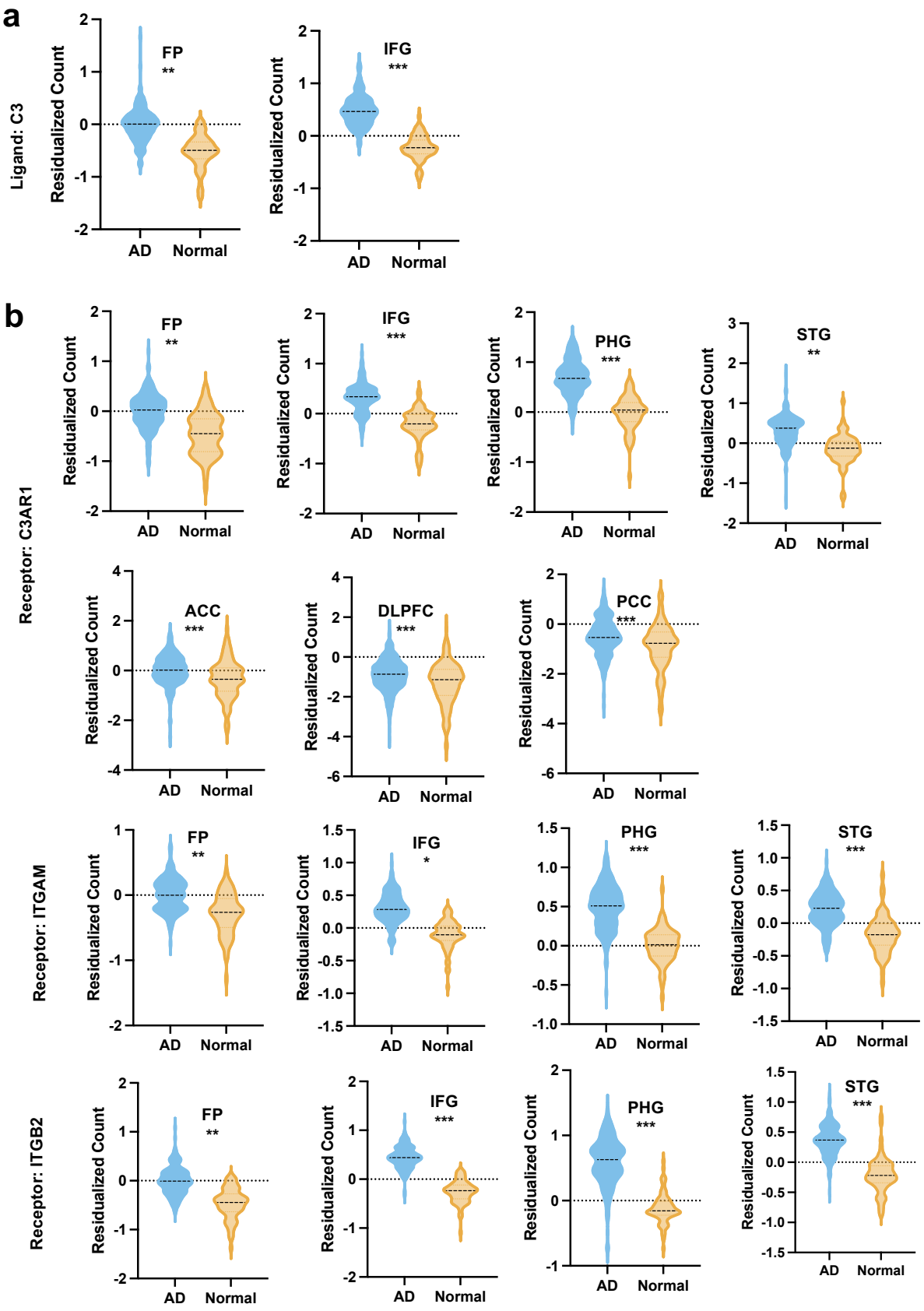

Supplemental Figure S18. Differential Expression of selected ligand and receptors involved in complement signal in bulk RNA-seq data (a). Ligand of C3 (AD vs, Normal, * q <0.05; ** q<0.01; *** q < 0.0001). FP: frontal pole; IFG: inferior frontal gyrus; **(b).** Receptors of C3AR1, ITGAM and ITGB2. TC: temporal cortex; FP: frontal pole; IFG: inferior frontal gyrus; PHG: parahippocampal gyrus; PC: prefrontal cortex; STG: superior temporal gyrus: DLPFC: dorsolateral prefrontal cortex; FC: frontal cortex.